2001

Comparison of Statistical and Model-Based Hindcasts of Subtidal Water Levels in Chesapeake Bay

Kathryn Thompson Bosley
Old Dominion University

Kurt W. Hess

Original Publication Citation

Bosley, K. T., & Hess, K. W. (2001). Comparison of statistical and model-based hindcasts of subtidal water levels in chesapeake bay. *Journal of Geophysical Research: Oceans, 106*(C8), 16869-16885. doi:10.1029/2000jc000237

JOURNAL OF GEOPHYSICAL RESEARCH, VOL. 106, NO. C8, PAGES 16,869–16,885, AUGUST 15, 2001

Comparison of statistical and model-based hindcasts of subtidal water levels in Chesapeake Bay

Kathryn Thompson Bosley

Center for Operational Products and Services,
National Ocean Service, NOAA, Old Dominion University Norfolk, Virginia

Kurt W. Hess

Office of Coast Survey, National Ocean Service, NOAA, Silver Spring, Maryland

Abstract. Subtidal water levels in Chesapeake Bay, which can have amplitudes as large as 1 m at Baltimore, are an important component of total water levels. The most importance forcing mechanisms for these variations are surface winds over the Bay and coastal subtidal water levels. Two methods for hindcasting subtidal water levels in the Bay were developed: statistical prediction (based on multiple linear regression) and a barotropic numerical circulation model-based prediction. The hindcast water levels were compared with the observed values at three key locations (Chesapeake Bay Bridge Tunnel (CBBT) in the lower bay near the mouth, Solomons Island at midbay, and Baltimore in the upper bay) by a variety of statistical measures. The hindcast results show that in both annually averaged differences and in the incidence of outliers the numerical model-based hindcasts are slightly more accurate than the statistical hindcasts, although on a monthly basis the statistical hindcast was often equal to or better than the model hindcast. Errors in both methods follow a seasonal pattern, being smallest in the summer months and largest in winter. Both hindcast methods explain significant portions of the observed variance. In addition, several techniques were used to estimate the relative importance of coastal water level forcing and wind forcing in the subtidal variability. In general, the two forcings were about of equal importance at Baltimore, while coastal forcing was dominant at Solomons Island and CBBT.

1. Introduction

Mariners operating in the Chesapeake Bay presently employ traditional National Ocean Service (NOS) tidal predictions, which are based solely on astronomical forcing. However, subtidal (i.e., with a frequency lower than ~ 0.95 cycles per day (cpd), the diurnal tidal frequency) variability is significant in the bay and at times the subtidal signal completely overwhelms the tidal signal (Figure 1). Therefore, for safety reasons, methods of hindcasting and eventually predicting subtidal variations are needed. Subtidal variations in water levels have been linked to two primary causes: direct (or local) wind forcing on the bay and a coastal (or remote) long wave that enters at the bay's mouth and propagates up the bay. For example, wind setup due to longitudinal north-south wind stress acting directly on the bay was identified as an important factor in producing subtidal water level fluctuations at Baltimore and Solomons Island, Maryland, by *Pollak* [1957, 1960]. In a series of papers examining subtidal water levels and currents in the bay and the Potomac River, D.P. Wang and A.J. Elliot [*Elliot*, 1978; *Wang and Elliot*, 1978; *Elliot and Wang*, 1978; *Wang*, 1979a, 1979b] found that the bay exhibited a response at 2- to 5-day periods, which was correlated to longitudinal wind forcing and possibly seiching at the bay's natural period. They also found that the response at longer periods (10 days or more) was correlated to longitudinal winds just outside the bay's mouth, implying Ekman transport from the local shelf. Additionally, for intermediate periods the bay's response was correlated to lateral (east-west) wind stress, implying forcing by coastal setup. *Wang* [1979c] found that the coherence between subtidal water fluctuations at the bay's entrance and nearby winds was relatively low but that coherence with subtidal water levels at Sandy Hook, New Jersey, was high, especially for periods > 3.3 days. On the basis of observed phase lags he concluded that the southern Middle Atlantic Bight was strongly influenced by free shelf waves generated north of Cape May, New Jersey, which propagated southward at a speed of 600 km d^{-1}. In Chesapeake Bay, water density distribution and stratification have been shown to have a strong influence on currents [*Wang*, 1979b; *Vieira*, 1986] but only a minor role in determining water level variability [*Blumberg*, 1978].

In an effort to hindcast these variations, we applied two common approaches: (1) statistical prediction equations derived by linear regression and (2) numerical circulation modeling. Statistical predictions based on multiple regression have been widely used in coastal forecasting. A statistical hindcast equation for water levels at Chesapeake Bay Bridge Tunnel (CBBT), using three variables (two wind stress components and atmospheric pressure) at a single location

Paper number 2000JC000237.

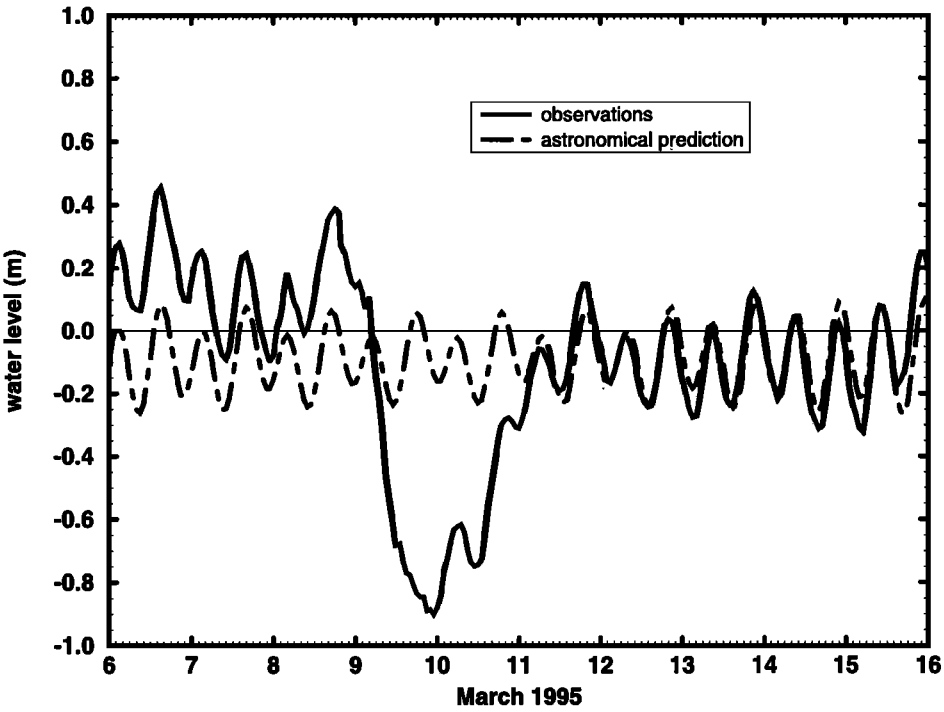

Figure 1. The observed (solid line) and astronomically predicted (dashed line) water level at Baltimore during a winter storm in 1995. A subtidal water level event appears as a rapid drop in water level during March 9-11. This draining of Baltimore Harbor was caused by the storm's strong northwesterly winds.

(CBBT), was developed by *Paraso and Valle-Levinson* [1996]. Their equation, developed with 1 year's worth of data (1992), was able to account for 58% of the total subtidal variability. A coastal forecasting method for water levels at several locations in Tampa Bay, Florida [*Zervas*, 1996], that incorporated a propagating shelf wave was based on a single variable, the subtidal water level observed several hours earlier at a station north of the bay's entrance. In our study, statistical hindcast equations were produced by correlating the variability of subtidal water levels in the bay with five variables, including two components of the wind stress at two locations inside the bay and the subtidal water level at a single coastal station outside the bay. Atmospheric pressure was not used. Hindcast equations were derived for three locations in the bay: Baltimore, Solomons Island, and CBBT.

A numerical model, driven by surface winds and a coastal setup, was the second approach used to generate water level hindcasts. Numerical circulation models of Chesapeake Bay have been designed for general or environmental hindcasting [*Blumberg*, 1977; *Johnson et al.*, 1990] and for process studies [*Spitz and Klink*, 1998]. Here we used the barotropic version of a three-dimensional model [*Hess*, 1989, 2000; *Johnson and Hess*, 1990; *Brooks*, 1994] which has been set up specifically for hindcasting and forecasting tidal and subtidal water levels in Chesapeake Bay [*Bosley and Hess*, 1998].

To determine accuracy, hindcast subtidal water levels from both methods were compared to the observations and each other at both monthly and annual timescales. We also compared properties of the hindcast subtidal water levels from both methods to the results obtained from other methods of analysis of the observational data, including empirical orthogonal function (EOF) analysis, to assess the relative importance of the direct wind forcing as compared to the coastal setup.

2. Data Sources

Six years (1991-1996) of hourly water level measurements from 10 NOS water level gauges within the bay were employed in this study (Figure 2). The gauges are located at Baltimore, Annapolis, and Solomons Island in Maryland and at Lewisetta, Gloucester Point, Sewells Point (Hampton Roads), Kiptopeke, and the Chesapeake Bay Bridge Tunnel in Virginia. With the exception of Kiptopeke, all the locations are on the south or west side of the bay. Data for only one station (Cambridge, Maryland) are available for this period, but this location is a ways up the Choptank River and does not adequately represent the bay. The lack of east side locations is not a severe limitation since the bay is quite narrow relative to its length and both the coastally forced long wave and the setup forced by over-bay winds vary primarily in the axial direction. Additional data from the same years for Lewes, Delaware, and Duck, North Carolina, were used to represent the coastal water level. The observational and harmonic constant data were obtained from NOS's Center for Operational Oceanographic Products and Services. In all cases, any missing data were filled in by standard NOS procedures which involve comparisons with nearby water level records and with tides predicted from the astronomical constituents. All 6 years of data were used in the EOF and spectral analyses, data from 1994 were used in developing each hindcast method, and data from 1996 were used to test each hindcast method.

Since water level records contain both the tidal and higher-frequency variations and the subtidal variation, the tidal signal was removed using two methods. Detiding, which is the subtraction of a astronomically predicted tide produced by employing the NOS harmonic constituents for each location, was most often used. The remaining signal consists primarily

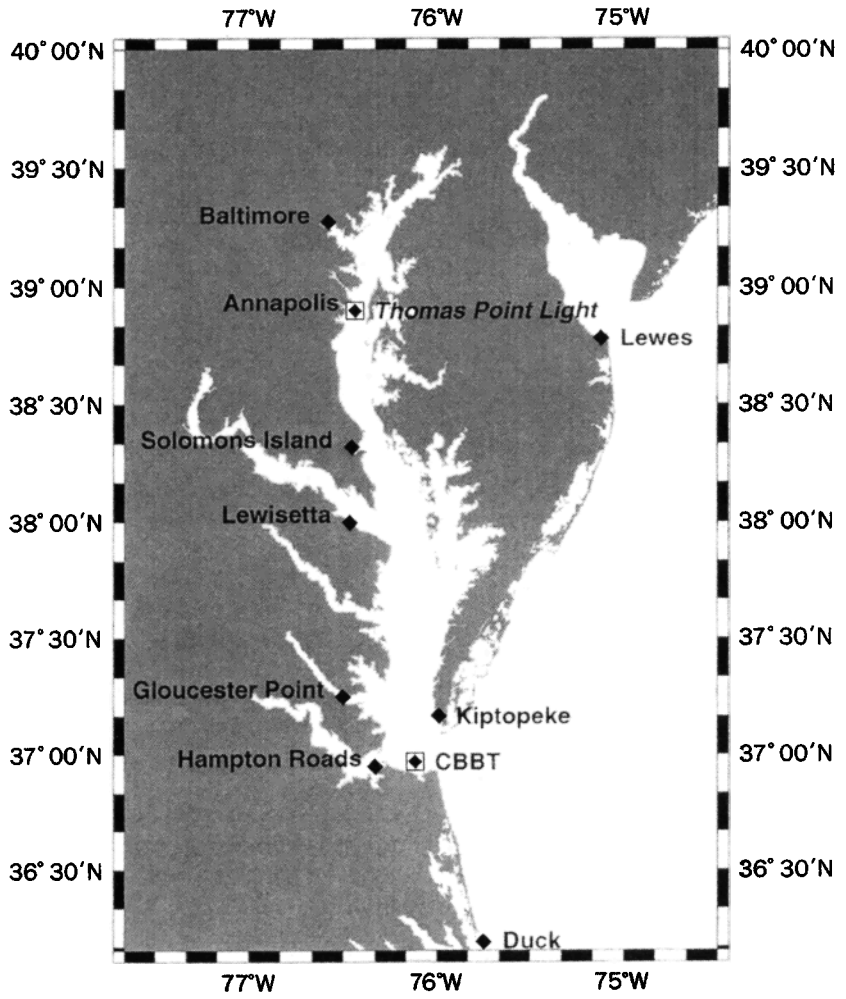

Figure 2. Location of the water level (diamonds) and wind stations (squares) used in this study.

of subtidal variations since the energy density at supertidal frequencies is at least an order of magnitude smaller than the subtidal energy density [*Paraso and Valle-Levinson*, 1996]. Low-pass filtering with a fast Fourier transform (FFT) with a 30-hour cutoff was used only to produce subtidal records for the EOF analysis. Signals were demeaned by subtracting the annual mean.

Hourly observations of wind speed and direction and barometric pressure for the years of 1991-1996 at the National Weather Service's (NWS) National Data Buoy Center's Coastal-Marine Automated Network (CMAN) station at Thomas Point and at the NOS meteorological station at CBBT were utilized to provide a measure of the wind field affecting the bay (Figure 2). All the data were used in the spectral analysis, data from 1994 were used in developing each hindcast method, and data from 1996 were used to test each hindcast method. For 1994 and 1996, there were relatively few gaps in the data. In addition, the analysis of wind-forced variability (section 6) gave remarkably similar results for the two years. Gaps in the wind record, which represent <2% of the total number of observations, were filled in two ways. If the gap was 6 hours or less, the missing northward and eastward speeds were filled by linear interpolation. If the gap was >6 hours, the missing components were filled with winds from the other station. NWS's assimilated wind fields, which are based on observations and the output of atmospheric models, could potentially provide greater spatial resolution, but they were available at a lower frequency (every 6 hours) than desirable.

River flows for the nine tributaries (the Susquehanna, Patuxent, Potomac, Rappahannock, York, James, Nanticoke, Choptank, and Chester Rivers) used in the numerical model were based on the monthly averaged values for flows from 1980 to 1994 determined by the U.S. Geological Survey. Flows at any particular time were obtained by linear interpolation of the monthly values. Since rivers flows were found to have only a very minor influence on water levels, it was decided that the use of data with a greater time resolution or data for 1996 was not necessary.

3. Characterization of Subtidal Water Level Variability

3.1. Qualitative Analysis of Subtidal Variability

The comparison of observed wind and detided water level signals at Lewes, CBBT, Solomons Island Baltimore in 1994 provided further insight into the nature and causes of the subtidal variability (Figure 3). We first note that the coastal water level signals at Lewes and CBBT for the whole year are

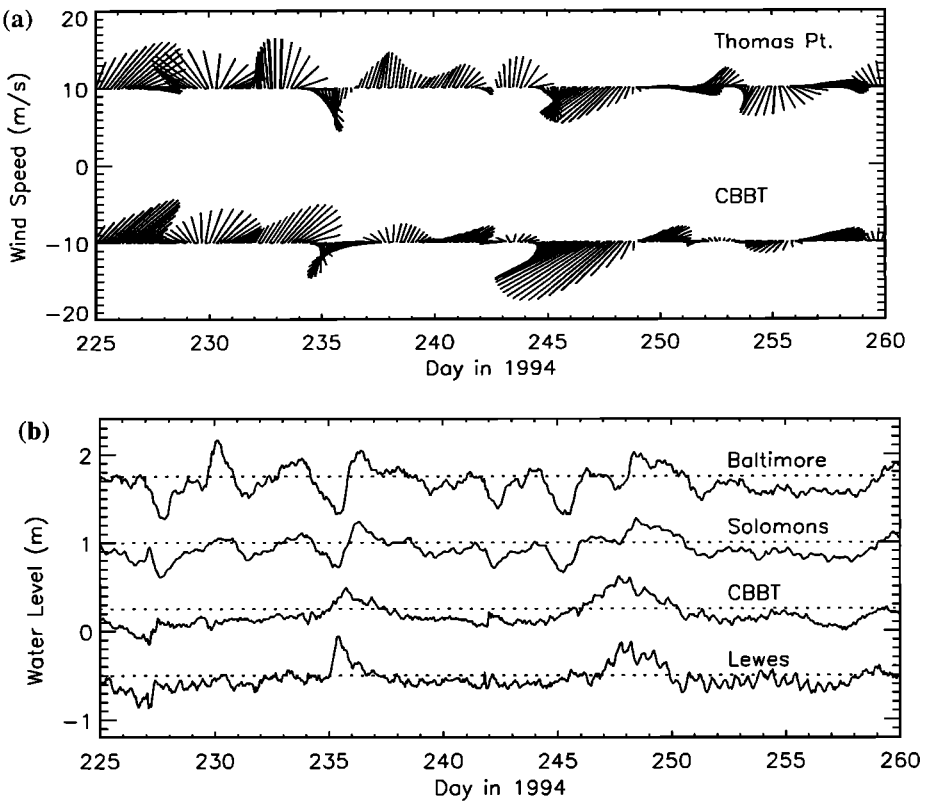

Figure 3(a). Filtered winds (showing direction toward which they are blowing) at Chesapeake Bay Bridge Tunnel (CBBT) and Thomas Point during a 35-day period in 1994. **(b)** Subtidal water level at four locations in the Chesapeake Bay region (Lewes, CBBT, Solomons Island and Baltimore) during a 35-day period in 1994. These data suggest that the subtidal signal at Baltimore is sometimes dominated by the effect of the undiminished coastal water level (e.g., days 248-250), by the effect of local wind over the Bay without a coastal influence (e.g., days 230-231 and 245), and by the effect of local wind which counteracts the coastal influence (e.g,. days 235-236 and 242). From the statistical equations the expected time lag from Lewis to CBBT is 8.7 hours, from CBBT to Solomons Island is 5.0 hours, and from Solomons Island to Baltimore is 6.8 hours.

remarkably similar in shape (correlation coefficient of 0.80) and amplitude (the standard deviation of the subtidal water level at Lewes was 17.7 cm and at CBBT was 17.0 cm). Assuming that the signal at CBBT or Lewes is an indication of the coastal forcing, some events, like that on days 248-250, can be classified as mostly coastal because the water level anomaly propagates up the bay virtually unchanged. On those and the preceding several days, strong and sustained winds from the northeast produced a large coastal setup. Other events have manifestations confined to the upper bay, such as those on days 230-231, when a large subtidal peak occurred at Baltimore and winds were gentle and rotated slowly from the southeast to southwest, and on day 245, when the small coastal subtidal signal is very different from the large changes in the signal at stations inside the bay. Winds at that time suddenly became strong and northeasterly. Finally, sometimes the effect of local wind is opposite that of the coastal influence. This occurred on days 235-236, when a large coastal setup occurred along with a large setdown in the bay while winds briefly became northerly, and on day 242, when a small coastal setup occurred with a small setdown in the bay while winds were variable but generally southwesterly.

Qualitative analysis of these individual events allowed us to hypothesize the physical causes of the occurrence and interaction of the observed subtidal variations as follows. Coastal subtidal waves enter the bay and travel up the bay with an amplitude that is relatively constant and with the same shallow-water gravity wave speed as the astronomic tide wave. The direct wind-driven water level response, which tends to have the opposite sign as the coastal wave, is strongly linked to both the direction and the duration of the winds. The most common wind systems are associated with the frequent passage of midlatitude atmospheric low-pressure systems across the bay, which move at a variety of speeds. In addition, because of the bay's extremely long north-south extent, winds in the lower bay can be different in speed and direction from those prevailing over the upper bay. Because of the bay's narrowness, even small differences in wind direction may give rise to significantly different responses. Depending on the arrival time at a particular location, the subtidal wave can often counteract the local wind effect. This partial compensation is the major reason that hindcasting bay subtidal water levels is so difficult.

3.2. Analysis of Subtidal Variability

3.2.1. Energy spectra. For water levels the amount of energy contained in the subtidal band varies with location from within the bay to out on the coast (Figure 4). In the 1- to 4-day synoptic band, Baltimore is most energetic, the midbay stations (represented by Solomons Island) contain less energy,

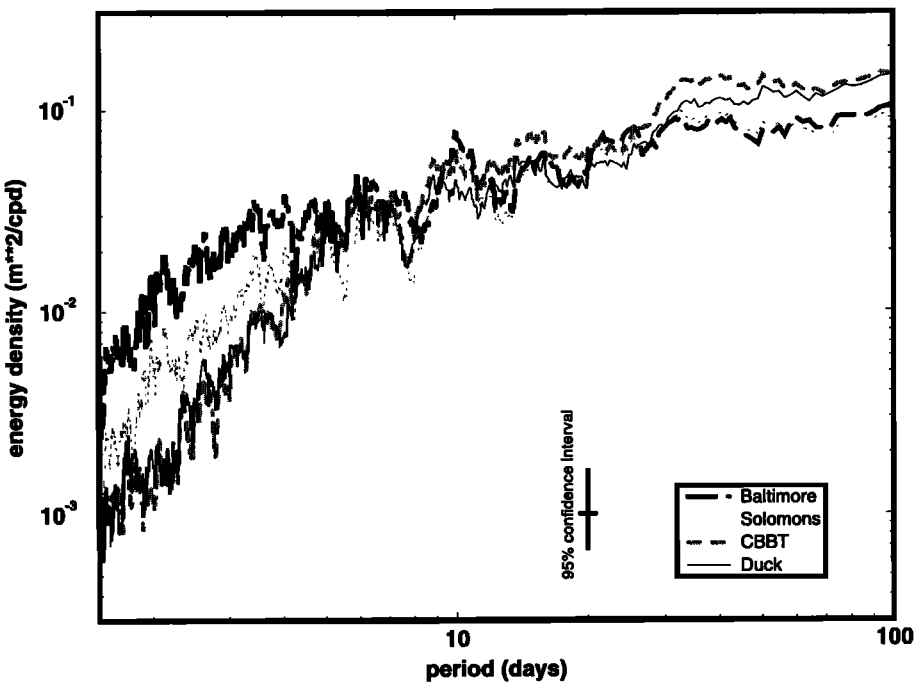

Figure 4. Spectra of energy in water level variations at three locations in Chesapeake Bay compared to the spectrum of energy on the coast at Duck, based on hourly water levels from 1991 to 1995.

and the coastal stations (CBBT and Duck) contain the least energy. In the long-period end of the spectra (periods >10 days), however, this trend is reversed; the coastal areas exhibit a great deal of energy, whereas Baltimore and the midbay are relatively less energetic. These results are similar to those obtained by *Wang and Elliot* [1978], for whom Annapolis was the most northerly water level station.

As noted by *Wang and Elliot* [1978], the similarities between the water level spectra and the wind spectra, especially in the 1- to 5-day band and the 10-day and above band, imply a strong connection between bay water levels and local winds. The fact that water levels at Baltimore are highly energetic in the 1- to 5-day band, even though winds in that band are less energetic, means that Baltimore either is influenced more by coastal forcing than local winds (i.e., the coastal wave is larger at Baltimore than at CBBT, which is not likely) or that Baltimore is exceptionally sensitive to local winds, even if they are weak. This second cause is more likely because winds can act on both the bay's long north-south axis and the local northwest-southeast axis from Baltimore Harbor to the entrance to the Chester River. Additionally, Baltimore Harbor is very shallow O(13 m).

3.2.2. EOF analysis. The EOF analysis of 30-hour low-pass filtered hourly water levels from 1991 to 1995 was employed to determine the geographic patterns and relative importance of the dominant modes of subtidal variability. The use of subtidal water level observations from four coastally influenced stations (CBBT, Kiptopeke, Lewes, and Duck) as well as the stations within the bay ensured the dominance of the coastal effect in the first mode. In terms of total energy the first two modes were the most important; the sum of the first and second modes accounts for from 97 to 99% of the total subtidal energy at all stations inside the bay as well as 82% at Lewes and 93% at Duck. Physically, the first mode represents the portion of the subtidal signal that is common to all 10 locations; in other words, it is a time series of bay and coastal water level rising and falling in unison. The amplitude of the first mode is relatively uniform over the bay, indicating that the effect of coastal water level is neither attenuated nor amplified by the bay (Figure 5). Although the amplitude of the first mode is nearly constant, the portion of the total subtidal water level that it explains varies within the bay. At Baltimore the first mode accounts for 58.1% of the subtidal energy (Figure 6). In contrast, at Solomons Island in the middle bay the first mode accounts for 85.0% of the energy, and at CBBT near the mouth of the bay the first mode accounts for 83.3% of the subtidal energy.

The second mode may be thought of as tilting of water levels along the axis of the bay and is generally considered to result from the direct effect of wind over the bay. The second mode accounts for only 15.8% of the energy at CBBT and 14.1% at Solomons but represents 40.9% of the energy at Baltimore. The amplitude of the second mode also varies within the bay; it is highest near the head at Baltimore, diminishes toward Lewisetta near the middle bay, and changes sign and then increases in amplitude toward the mouth. This change in sign between the upper and lower bay indicates that a node is located between Gloucester and Lewisetta. Because the amplitudes are approximately equal in magnitude at these two locations, we estimate that the nodal line is located midway between them. This location is at about one-fourth of the distance from the entrance to the head at the Susquehanna River. Theory says that for an enclosed basin with uniform width and depth the nodal line would be about at the halfway point [*Hutchinson*, 1957]. However, since the southern half of the bay is wider than the northern half, the nodal line would be positioned more to the south, and since the bay is open at its southern end, the position of the nodal line would be further modified. Friction would also alter the node's position. These patterns of variability support the concept of a coastal signal having a uniform importance throughout the bay (as shown in the EOF first-mode amplitudes) and the increasing importance

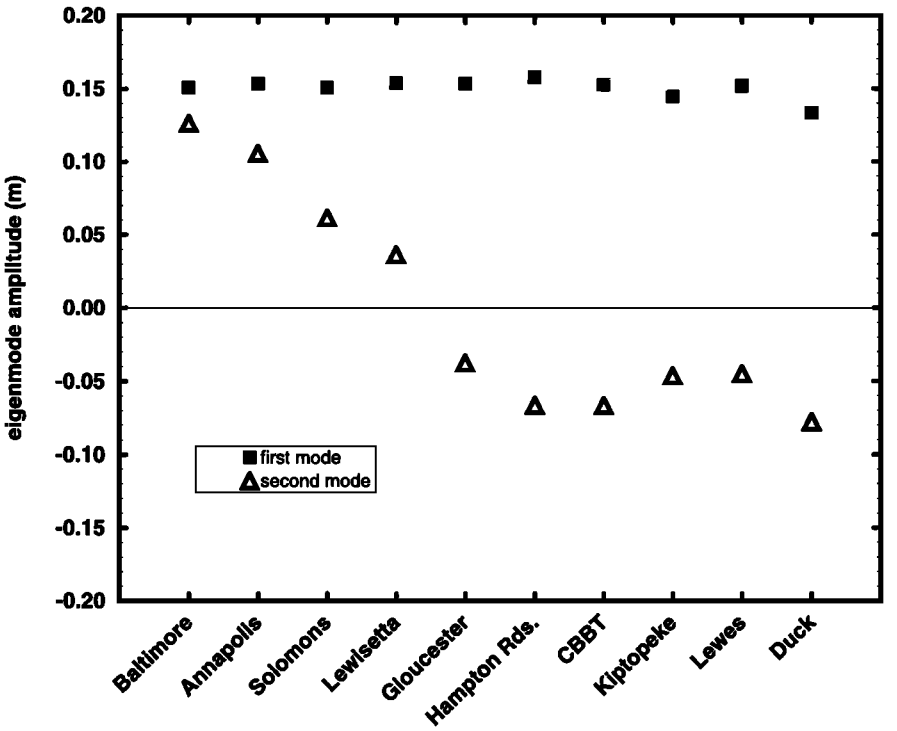

Figure 5. Amplitude of the eigenvectors of the first two modes of an empirical orthoganal function (EOF) analysis for locations within the Chesapeake Bay area, based on hourly water levels from 1991 to 1995.

of the direct wind effect in the upper bay (as shown in the EOF second mode and the water level spectra).

3.2.3. Analytical model. *Garvine* [1985] developed a set of analytical equations for water level and velocity in an idealized bay of constant width and depth which were forced by a spatially uniform wind stress and a coastal elevation change (with magnitude proportional to the wind stress). He found a solution that varied with time at constant frequency (corresponding to a period of 7 days). He compared the amplitude of the coastal and wind-forced terms in the solution

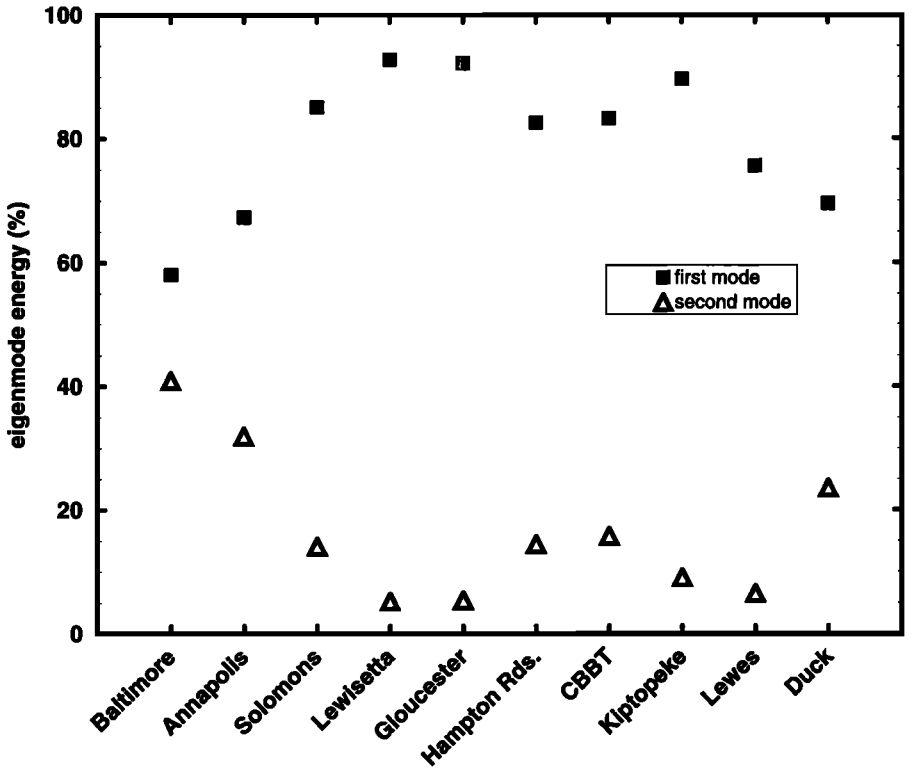

Figure 6. Percentage of the variability contained in the first two modes of an EOF analysis for locations within the Chesapeake Bay area, based on hourly water levels from 1991 to 1995.

for total water level and found that the component forced by coastal setup is approximately uniform throughout the bay. However, the wind effect was proportional to the distance from the entrance. Thus, at small distances (i.e., near the mouth) the coastal effect, whatever its magnitude, would dominate. Wind effects would be small but become more important with distance from the entrance. Although he did not make any calculations directly relating to Chesapeake Bay, Garvine notes that if an estuary is oriented nearly parallel to coast, as is the Chesapeake Bay, the two effects would act in opposition.

Although the spectral, EOF, and analytical model analyses described above provide considerable information on the bay's subtidal water level variability and its relation to coastal water level and local wind forcing, none of these approaches can be easily used for hindcasting. This is because the spectra have no time dependence, the EOF results are not directly related to the wind signal, and the analytic method does not allow width, depth, or wind to vary in space. Thus we proceed to the statistical correlations and numerical hydrodynamical modeling as the hindcast methods for this study. On the basis of the previous analyses the strategy of the study was to use three stations (CBBT, Solomons Island, and Baltimore) as proxies for the entire bay.

4. Statistical Hindcasts

4.1. Indicators of Coastal Forcing

To select an indicator of coastal forcing, we used cross-spectral analysis of subtidal water levels inside the bay and water levels at a number of coastal stations up and down the coast outside of the Chesapeake Bay entrance. For the subtidal water level at Baltimore, cross-spectral analysis was performed with the subtidal water levels observed in 1994 at CBBT, Duck, and Lewes. The coherence between Baltimore and each of these three coastal stations is only significant for periods >4 days. Baltimore is most coherent with Lewes, which is interesting, given that CBBT and Baltimore have the Chesapeake Bay in common, while Lewes is in the Delaware Bay. It may be that Baltimore and Lewes are affected similarly by the winds of storm systems which transit the area because they are located at about the same latitude. In addition, they are both located in shallower water than CBBT is. For Solomons Island, a statistical predictor of the coastal effect was sought using subtidal water level observed at CBBT, Lewes, and Duck. Again, of the three coastal sites the coherence with Lewes was the highest. However, unlike the situation at Baltimore, the coherence remains significantly high even for periods as short as 2 days.

For CBBT, only Lewes and Duck were investigated as indicators of the coastal effect. In contrast to the results at the two locations inside the bay, subtidal water levels at CBBT are slightly more coherent with those at Duck than with those at Lewes. The coherence between the two signals is significant in both the subtidal and tidal frequency ranges. Unfortunately, the time lag between Duck and CBBT is only on the order of 1 hour, thus making Duck an unsuitable choice for a predictor. Therefore subtidal water levels at Lewes (which lead water levels at CBBT by several hours) were selected for the predictor of coastal forcing in the regression equations.

4.2. Indicators of Wind Forcing

To choose an indicator of wind forcing, we performed cross-spectral analysis between the subtidal water level records from each of the three locations in 1994 and the wind stress observed at both Thomas Point and CBBT along 18

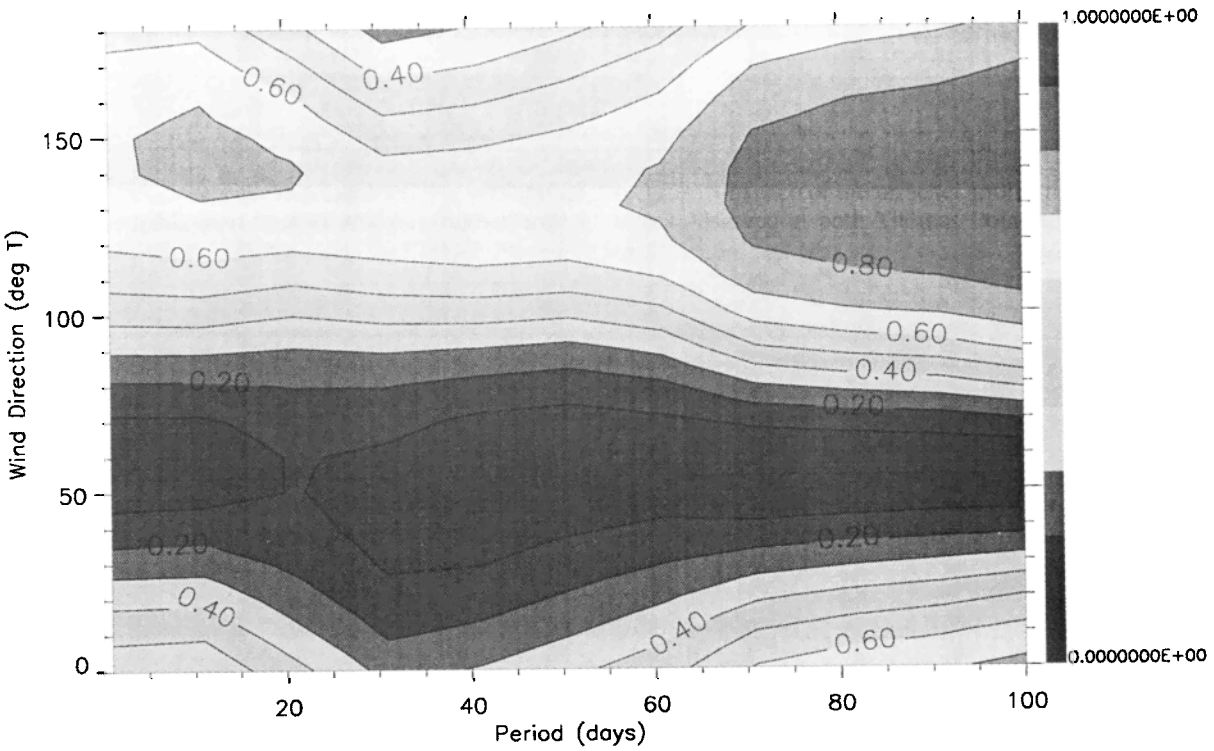

Figure 7. Coherence between the subtidal water level variation at Baltimore and the wind stress at Thomas Point as a function of wind direction (from) and period. For synoptic periods (1-20 days), coherence is highest at 140°, or winds from the southeast. Coherence is based on hourly winds from 1994.

uniformly spaced directions from 0° to 170°. For each location in the bay and for each of the two wind sensor locations we elected to use the wind direction which produces the most coherence with the subtidal water level.

At Baltimore the subtidal water level is most coherent with the wind stress observed at Thomas Point, which is oriented along (and based on winds from) 140° (Figure 7), and wind stress from 140° at CBBT. This very interesting characteristic may stem from the fact that this orientation represents the approximate axis of Baltimore Harbor. The harbor is shallow, and thus water level there is very sensitive to wind blowing along its axis. The subtidal water level at Solomons Island is most coherent with stress from winds from 130° at Thomas Point and from 50° at CBBT. The wind observed at CBBT has the most effect on the subtidal water level in the lower Bay at CBBT. The signal is most coherent with wind blowing from 50° at CBBT and from 50° Thomas Point.

4.3. Hindcast Equations

On the basis of multiple linear regression and the predictors for coastal and wind forcing selected above the statistical prediction equations for subtidal water level relative to annual mean sea level (MSL) are as follows. For Baltimore,

$$\eta'_B(t) = 0.700\eta_L(t - 15.48) + 0.868\,\tau^*_{T140}(t - 7.46) + 1.023\tau^*_{C140}(t - 9.49); \quad (1)$$

for Solomons Island,

$$\eta'_S(t) = 0.705\eta_L(t - 13.68) + 0.357\,\tau^*_{T140}(t - 8.55) + 0.844\tau^*_{C130}(t - 8.52); \quad (2)$$

and for CBBT,

$$\eta'_C(t) = 0.722\eta_L(t - 8.66) + 0.018\,\tau^*_{T050}(t - 10.98) + 0.747\,\tau^*_{C050}(t - 1.48), \quad (3)$$

where η' is the hindcast water level, η_L is the observed subtidal water level relative to MSL at Lewes (all water levels have units of meters), time t is in hours, and τ^* is the wind stress per unit density ($m^2 s^{-2}$). For the wind stress the subscript denotes either Thomas Point (T) or CBBT (C) and the direction from which the wind comes. For a wind of speed W the wind stress per unit density is calculated as

$$\tau^* = \rho_a(C_{a1} + C_{a2}W)\,W^2 \quad (4)$$

and is in the direction toward which the wind is blowing. The drag coefficients are $C_{a1} = 0.0008$ and $C_{a2} = 0.000065$ s m^{-1} [*Wu*, 1980], and the air density per unit density ρ_a is 1.2.

These equations support several points that were highlighted in the characterization discussion. The strength of the response to coastal setup/setdown is relatively constant throughout the bay as evidenced by the similar amplitude factors applied to subtidal water level at Lewes. Also note that the optimum time lags for water level response (13.68 - 8.66 = 5.02 hours for Solomons Island and 15.48 - 8.66 = 6.82 hours for Baltimore) increase with distance from the mouth, which is consistent with the progression of a shallow-water wave up the bay. In comparison, for a shallow-water wave in a mean depth of 10 m (and a speed of 10 m s^{-1}) a CBBT to Solomons Island distance of 140 km implies a time lag of 3.89 hours, and a CBBT to Baltimore distance of 240 km implies a time lag of 6.67 hours. These time lags indicate that in the lower bay a mean depth of 6 m (and a speed of 7.8 m s^{-1}) is more representative.

The wind stress terms present some interesting features. First, we note that in each individual equation the dominant wind angles at CBBT and Thomas Point, being at most 10° apart, are nearly identical. This indicates that the forcing winds are at the synoptic scale and that subsynoptic-scale wind effects are of minor importance. At Baltimore, nearly equal coefficients in the wind stress terms (which are both from the southeast) indicate that winds from the southeast at both stations will raise water levels an equal amount. At Solomons Island, southeast winds also raise the water level, but since the Thomas Point coefficient is only half the CBBT coefficient, the influence of upper bay winds is relatively less. At CBBT the dominant wind direction is from the northeast, indicating the importance of Ekman transport from the adjacent shelf; upper bay winds have a negligible effect there.

5. Model-Based Hindcasts

5.1. Numerical Model

The numerical code used to generate the hindcasts is the Model for Estuarine and Coastal Circulation Assessment (MECCA) [*Hess*, 1989, 2000; *Brooks*, 1994; *Johnson and Hess*, 1990]. The MECCA code solves the hydrodynamic equations of momentum, mass, salt, and heat conservation. The model is three-dimensional in space, uses a vertical σ coordinate, has a time-varying free surface, and incorporates nonlinear horizontal momentum advection. The model includes a time-variable horizontal diffusion coefficient based on the Smagorinsky approach [*Tag et al.*, 1979]; the coefficient is a background value (1 m^2 s^{-1}) plus the product of a constant (0.01), the square of the grid cell size, and the square root of the sum of the squares of the horizontal velocity gradients. Variables are placed on an Arakawa C grid with square cells in the horizontal and at uniform intervals along a σ-stretched vertical coordinate. The external-mode momentum equation is solved with an alternating-direction, semi-implicit method in the horizontal. The finite difference equations conserve mass and salt for a variety of boundary conditions. For this application the model is run in the barotropic mode because sensitivity studies of Chesapeake Bay response incorporating the three-dimensional currents and constant density showed little difference from the two-dimensional results for water levels and because adding stratification will not significantly alter the synoptic-scale response of the water levels [*Blumberg*, 1978]. The grid measures 55 by 34 cells (Figure 8) with a cell size of 5.6 km and uses bathymetry developed at the U.S. Naval Academy (M. Hoff, unpublished report, 1990), with a minimum cell depth of 1 m and maximum depth of 19 m. Upper reaches of rivers are modeled as narrow channels. Triangular cells contain the same placement of variables but have half the cell area of a square cell. The present grid size covers the bay's north-south extent, which corresponds to the approximate length of the tide wave [*Browne and Fisher*, 1988], with 50 cells. Also, since the east-west slopes of the major tidal constituents are relatively uniform over the bay's width [*Browne and Fisher*, 1988], the 5.6 km grid is probably fine enough to capture most of the water level variability. In addition, test runs with cell dimensions half of the present size showed little difference in simulated water levels, indicating that changes in water level slopes over distances of the order of 5 km are probably not significant.

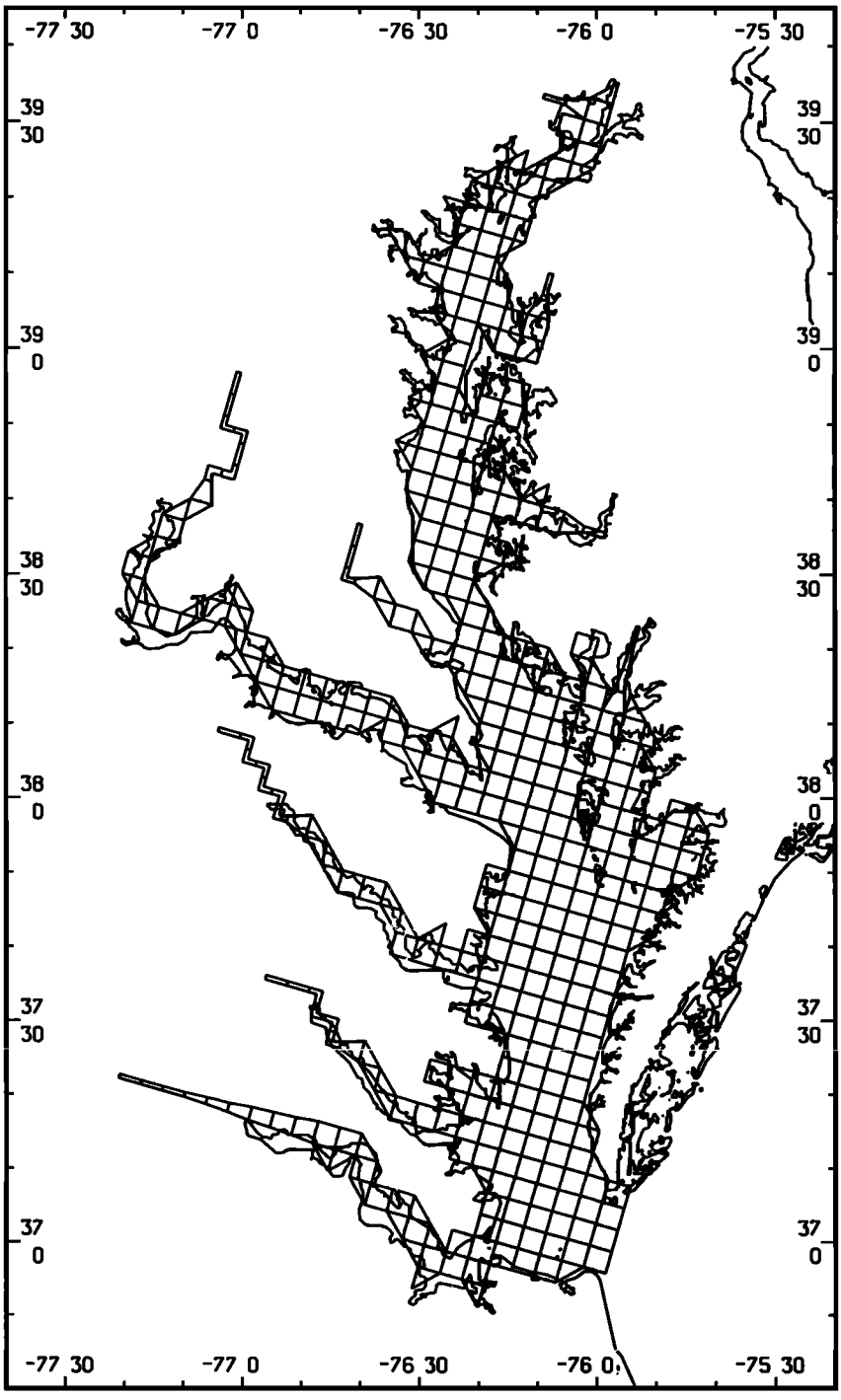

Figure 8. Locations of water level computation points (Triangles and squares) at the center of cells in the MECCA model grid for Chesapeake Bay. Grid cells are 5.6 km on a side. The squares show the location of the cells representing the three proxy stations.

5.2. Boundary Conditions

For the continental shelf boundary in the hindcasts, the subtidal water level at the shelf open boundary used to drive the model η'_O is computed from the observed total water level relative to MSL at CBBT η_C by applying an amplitude correction factor α and a time correction γ as follows:

$$\eta'_O(t) = \alpha\eta_C\,(t+\gamma) \tag{5}$$

For the hindcasts that included remote forcing, h_C was the observed water level (which includes the tides) relative to MSL. For the astronomical tide only forcing, η_C was reconstructed using NOS amplitude and epoch values for 29 tidal constituents. The values of α and γ were established during the calibration process (see section 5.3). These parameters account for the fact that CBBT is located three grid cells into the model domain rather than at the true open boundary. The

Table 1. Comparison of the Predicted Astronomical Tide (Relative to Mean Sea Level) and the Demeaned, Numerically Modeled Astronomical Tide at Several Locations in Chesapeake Bay, Based on 365 days of Hourly Values for 1994.

	Location						
	CBBT	Kiptopeke	Gloucester	Lewisetta	Solomons	Annapolis	Baltimore
RMS, cm	0.7	2.6	4.7	3.9	4.8	5.0	6.4
RAE, %	1.1	4.2	8.8	12.6	16.3	19.7	22.7
CC	1.000	0.998	0.989	0.978	0.950	0.935	0.913

Quantities shown are the RMS of the differences (cm), the relative average error (RAE) as a percent, and the correlation coefficient (CC). RAE is the sum of the absolute values of the hourly differences divided by the sum of the absolute values of the hourly predicted values and the absolute values of the modeled values [*Willmott et al.*, 1985].

difference between MSL at the two locations was assumed to be zero. Kiptopeke was also considered for the boundary condition, but because it is located on the north side of the entrance and adjacent to the shallower of the two natural channels, CBBT was thought to be more representative of water level variability on the shelf.

At the water-bottom interface, the bottom stress τ_b is expressed as

$$\tau_{bx} = \rho C_{b1} u_x \qquad \tau_{by} = \rho C_{b1} u_y , \tag{6}$$

where ρ is water density, C_{b1} is a drag coefficient, and u_x and u_y are the depth-averaged velocities in the x and y directions of the model's coordinate system, respectively. Thus the bottom stress is assumed to be a linear function of the velocity. The value of C_{b1} was established during the calibration process (see section 5.3).

Wind stress at each model cell is calculated from the wind using the same air density and drag coefficient as in (4). Wind fields for the hindcasts were generated from the hourly observations at CBBT and Thomas Point as follows. In the northern part of the bay (north of 38°30'), northward and eastward components of the wind are set equal to those components at Thomas Point, and in the southern part of the bay (south of 38°00'), northward and eastward components of the wind are set equal to those components at CBBT. In the remaining middle bay, each wind component is linearly interpolated in space between the southern and northern values. Tests conducted as part of the Coastal Marine Demonstration Project [*Walstad et al.*, 2000] show that the use of higher-resolution wind fields does not significantly improve model accuracy.

River flow rates are applied by a mass-conserving, a "waterfalls" condition at the upper reaches of nine tributaries. For the boundary condition an incremental elevation, equal to the product of the flow rate, the time step, and the inverse of the cell area, was added at the end of each time step to the model-computed water level in the designated river cell. Flow rates for any given time were determined by linear interpolation between the monthly mean values.

5.3. Calibration and Validation

Calibration was a two-step process consisting of preliminary and final calibration. During preliminary calibration the

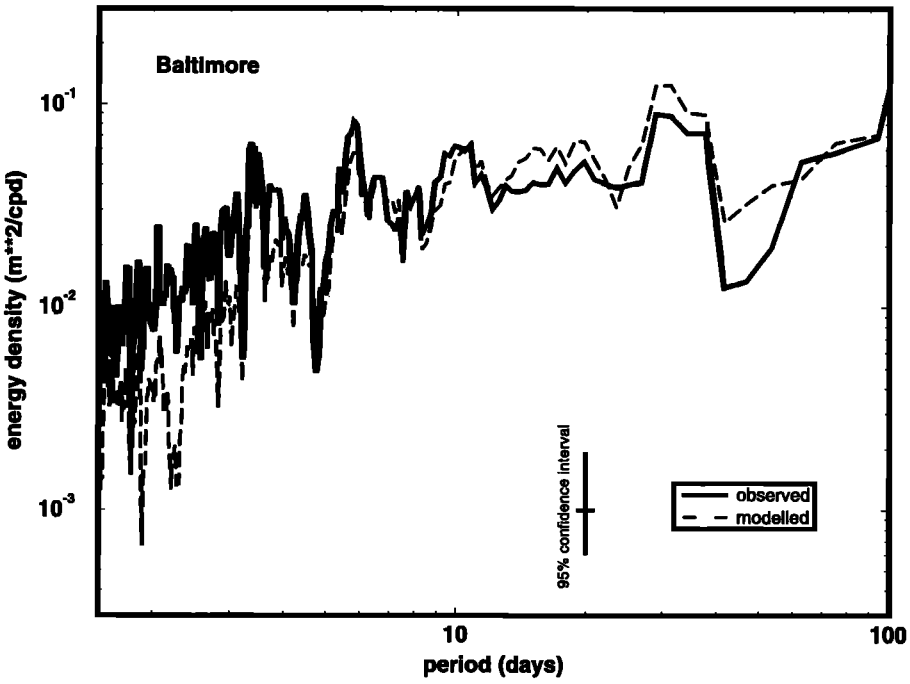

Figure 9. Spectral energy of the observed and modeled water level at Baltimore, based on hourly data for 1994.

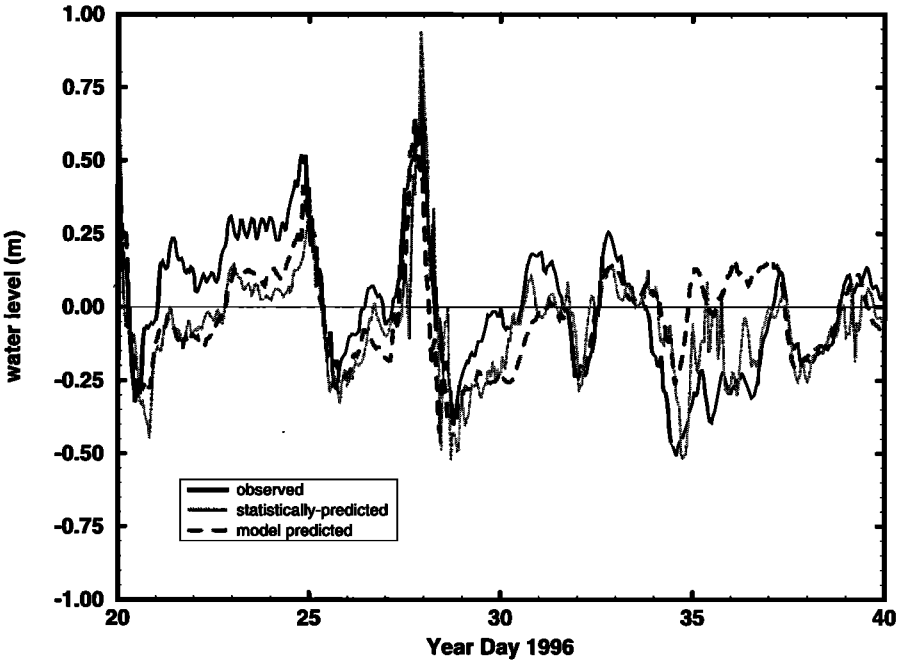

Figure 10. Demeaned subtidal water levels at Baltimore for a 20-day period in 1996. The observed (solid line), statistically predicted (dotted line), and model-predicted (dashed line) water levels are shown. Both predictions capture many of the major fluctuations but miss some of the smaller fluctuations.

model was forced with astronomical tide and monthly mean river flow only, and a small depth value δ was added to the MSL water depth at each cell to correct the phase of the astronomical tide at Baltimore. With δ fixed the parameters α, γ, and C_{b1} were adjusted iteratively to give the best match (i.e., the minimum RMS difference) between modeled and predicted (astronomical tide only) hourly water levels at 10 bay stations for 2 months (October and November 1994). During each iteration of the adjustment, first, C_{b1} was held fixed and α and γ were adjusted to find a best fit, then, C_{b1} was adjusted with α and γ held fixed. In the final calibration the model was forced with the observed total water level, spatially interpolated hourly winds, and monthly mean river flow. The parameters α, γ, and C_{b1} were readjusted iteratively as described above to give the best match to hourly total observed water levels at the same 10 bay stations and time period as the preliminary calibration. The results for the water level parameters were α = 1.013, indicating that the water levels on the shelf had larger amplitudes, and γ = 0.17 hours, indicating that the phase on the shelf was several minutes earlier. The result for the bottom drag coefficient was $C_{b1} = 0.0007$ m s^{-1}.

The model was validated using three methods. The first method involved running the model for the entire year of 1994 with only the predicted astronomical tide at the mouth and harmonically analyzing the water levels at three stations. The tidal constituent amplitudes and phases were then compared to the accepted NOS values. The results showed excellent agreement between the model and the NOS values for the six most dominant constituents (M_2, S_2, N_2, K_1, O_1, and P_1). At CBBT the largest amplitude difference was only 0.1 cm with a maximum phase difference of 2°. At Baltimore the agreement was also excellent, with maximums of 1.8 cm and 8.8°. Results were only slightly less accurate at Solomons Island. The next method of validation was the comparison of the hourly water levels (from the year-long astronomical tide run) at several Bay stations. The RMS differences, which are generally small, are shown in Table 1. The difference at CBBT, near the entrance, is the lowest (0.7 cm) and generally increases with distance up the bay. The largest value (6.4 cm)

Table 2. Comparison of the Difference Between the Hindcast and the Observed Subtidal Water Levels at Three Locations in Chesapeake Bay.

Location	RMS Difference, cm				Percentage of Outliers			
	Statistical Hindcast		Model Hindcast		Statistical Hindcast		Model Hindcast	
	1994	1996	1994	1996	1994	1996	1994	1996
Baltimore	10.5	13.4	10.1	12.1	1.38	3.56	0.70	0.58
Solomons Island	7.8	9.2	7.7	9.1	0.29	0.82	0.22	0.42
CBBT	6.8	7.4	2.8	2.8	0.24	0.42	0.00	0.00

Data are the hourly values from 1994 (calibration) and 1996 (validation). Outliers are the percentage of the differences whose absolute value was equal to or greater than 30 cm.

occurred at Baltimore. The final method of validating the model was to compare the power spectra of the observed and simulated water levels. The results for Baltimore are shown in Figure 9. Overall, the spectrum of the observed data is matched by the model. Differences occurring in the 1.5- to 5-day period band suggest that the model is not energetic enough in response to direct meteorological forcing. This may be attributed to the lack of spatial (and temporal) resolution in the driving wind fields.

6. Analysis Of Hindcast Results

Using the statistical equations and numerical model (which were calibrated using 1994 data for hourly winds at CBBT and Thomas Point and hourly water levels at CBBT and data from 1980 to 1994 for monthly mean river flows), we made two year-long hindcasts for 1996 using that year's winds and water levels and the same monthly mean river flows but not changing the coefficients in either set of hindcast equations. For comparison purposes, we also ran both methods to produce hindcasts for 1994 using that year's data for input. The simulated water levels were saved at 1 hour intervals. The numerical model's subtidal water level was generated by subtracting the hourly values of a year-long run forced with astronomical tide and river flow only from a year-long run forced by astronomical tide, river flow, wind, and coastal setup. Sample hindcasts of the subtidal water levels at Baltimore during 1996 using both methods are shown in Figure 10. In general, both predictions capture many of the major fluctuations in the observed signal but miss some of the smaller fluctuations. This is probably due to the fact that the statistical and the numerical model predictions are limited because they are based on only three observed input variables, simple relationships with fixed coefficients which were used to generate the boundary input values from the observed values, and (for the model) cell depths which may have introduced errors in long-wave propagation speeds.

6.1. Annually Averaged Accuracy

We first examined the relative accuracy of each hindcast method in reproducing the observed subtidal water level variation at three stations (Baltimore, Solomons Island, and CBBT). When averaged over the year, the model gave lower differences at all locations and for both years (Table 2). Another statistic useful to navigation is the percentage of time that the hindcast water level differed from the observed by more than a specified limit (30 cm); this statistic is termed the outlier percentage [*NOS*, 1999]. The percentage of outliers for the model-based hindcasts is also lower than for the statistical hindcasts. This fact is particularly true at CBBT since the model is forced at the open boundary with CBBT observations.

Two other interesting trends are evident in these comparison data. First, there is a general tendency toward lower accuracy in the hindcasts as distance from the entrance increases. That is, both the RMS differences and percentage of outliers (model and statistical) are lower at CBBT than at Baltimore. This behavior is consistent with the fact that the locations become more distant from the location of the coastal forcing station. Second, the results for the calibration year (1994) are in general better than for those for 1996. This finding is the rather obvious result of the exclusive use of 1994 data both to derive the statistical equations and to calibrate the model.

Using the 1996 data, we estimated the predictability of each method as measured by the reduction of variance. At Baltimore the initial variance of the subtidal water level was 400.1 cm^2 (Table 3). When the subtidal water level as hindcast by the statistical equation is removed, the variance of the remainder is 179.6 cm^2, or 44.9% of the original. Thus the subtidal water level as modeled by the statistical equation explains 55.1% of the variability at Baltimore. Similarly, at Solomons the statistical hindcast explains 66.2% of the variability, and at CBBT it explains 78.6% of the variability. For comparison, using statistical regression techniques, *Elliot* [1978] was able to explain ~50-60% of the variance in Potomac River currents, and *Paraso and Valle-Levinson* [1996] were able to explain ~58% of the subtidal sea level variability at CBBT. For the model-based hindcasts, when the subtidal water level predicted by the model is removed from the observed, the variance of the remainder at Baltimore is 146.4 cm^2, or 36.6%. Thus the model hindcast explains 63.4% of the variability. Similarly, at Solomons the numerical model explains 67.1% of the variability, and at CBBT, the numerical model explains 97.0% of the variability. Therefore the numerical model explains, on the average, 9% more of the total variance than does the statistical model.

6.2. Seasonal Variation of Accuracy

Further insights can be gained by examining changes in the RMS differences between the predicted and the observed subtidal water level and the outlier percentages as they vary throughout the 1996 hindcast year. The hourly differences between the observations and hindcast values were binned by month, and then the monthly averaged values of RMS differences and outlier percentages were calculated. The RMS differences vary considerably throughout the year (Figure 11a). All three stations show a maximum in winter (December and January) and a minimum in summer (June to August). This pattern suggests that errors both inside of the bay and at the entrance are highly related to midlatitude wind events, which in 1996 (as in most years), were strong and frequent in the winter months and weaker and less frequent in the summer months. This finding is consistent with that of *Wang* [1979a],

Table 3. Variances and Percentages of the Observed for the Total (Observed) Subtidal Water Level and for the Remainder When the Statistical and Model-Based Hindcasts of Subtidal Water Level Have Been Removed.

Signal	Baltimore	Solomons Island	CBBT
Observed	400.1 (100.0%)	248.7 (100.0%)	252.6 (100.0%)
Observed minus statistical prediction	179.6 (44.9%)	84.1 (33.8%)	54.1 (21.4%)
Observed minus model-based prediction	146.4 (36.6%)	81.8 (32.9%)	7.7 (3.0%)

Data are for 1996. Note that the square root of the variances equal the RMS differences in Table 2. Variances are in cm2.

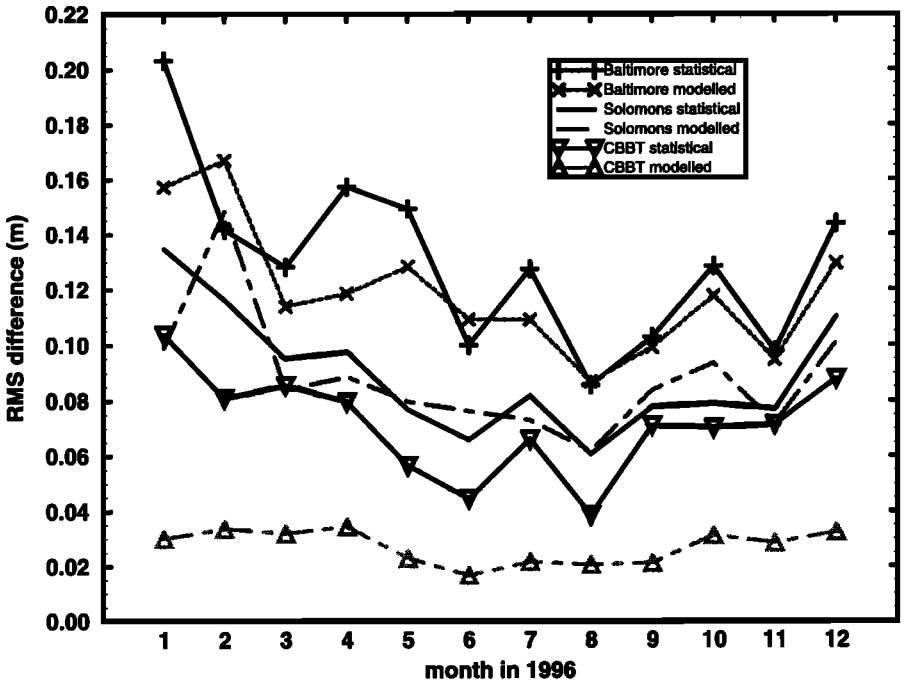

Figure 11a. Monthly variation of RMS difference between observed and hindcast subtidal water level for 1996.

who determined that barotropic current fluctuations were twice as large in winter than in summer.

Although the model produces lower RMS errors when averaged over the year at all stations for each year, only at CBBT is the model consistently better on a month-to-month basis. At the other locations the statistical hindcast was often equal to or better than the model hindcast. The fact that the model does so well at CBBT is, as stated above, due to the fact that the model is forced with observations of water level taken at CBBT, whereas the statistical method uses the water level at Lewes, located ~225 km up the coast.

The outliers also vary throughout the year (Figure 11b). As with the monthly RMS differences, all three stations show a maximum in winter (January and February) and a minimum in summer (June and August). This pattern suggests, as does the variation of RMS differences, that errors both inside and at the mouth of the bay are highly related to midlatitude wind events.

6.3. Hindcasts of Total, Coastally Driven, and Wind Driven Variations

A comparison of the subtidal variability in 1994 and 1996 due to (1) total forcing, (2) coastal setup forcing only, and (3) local wind forcing only was made to determine the ability of each hindcast method to separate the latter two signals. Although both hindcast methods were validated with 1996 data, the results for the 1994 data are included to assist in establishing spatial patterns. For each method the water level signal for total forcing was generated as explained in section 6.1 The statistical coastally forced signal was generated by simply rehindcasting water levels for the whole year but including the Lewes detided water level and excluding the wind terms. The statistical wind-forced water level signal was generated by including the wind terms while excluding the Lewes water level term. For the numerical model, several runs with different combinations of forcings were made because the presence of the nonlinear advective terms in the equations of motion produces interactions that make the determination of the response from a single forcing difficult to isolate. The numerical model's coastally forced water level was generated by subtracting the hourly values of water levels of a year-long run produced with astronomical tide and river flow as the only forcing from the hourly values a year-long run forced by astronomical tide, river flow, and coastal setup (but no wind). The numerical model's wind-forced water level was generated by subtracting the hourly values of water levels from a year-long run with astronomical tide and river flow as the only forcing from a year-long run forced by astronomical tide, river flow, and wind (but no coastal setup). The results for the variance using both methods and both years are shown in Table 4.

Several aspects of the results are noteworthy. First, for the total water level, there are significant differences between the variance of the hindcast and the variance in the observed. For the statistical hindcast the variance at all locations and in both years is less than the observed because linear regression does not account for all the observed variance. For the model-based hindcast the variance is higher than observed at CBBT, about the same at Solomons Island, and lower than observed at Baltimore (see Figure 9), possibly indicating errors in bottom friction or wave propagation.

Second, in both hindcast methods the variance in the coastally forced water level variation is remarkably uniform throughout the Bay. Spatial variation between results within each year and method is at most 6%. These results correspond with the findings of the EOF analysis of the observed water levels discussed in section 3. Figure 5 shows that the amplitude of the first mode (which corresponds to the coastally forced response) is exceptionally uniform, with an amplitude of ~16 cm (corresponding to a variance of 256 cm^2) throughout the bay. This uniformity is also consistent with the concept of a coastally forced long wave that propagates up the bay with little change in amplitude.

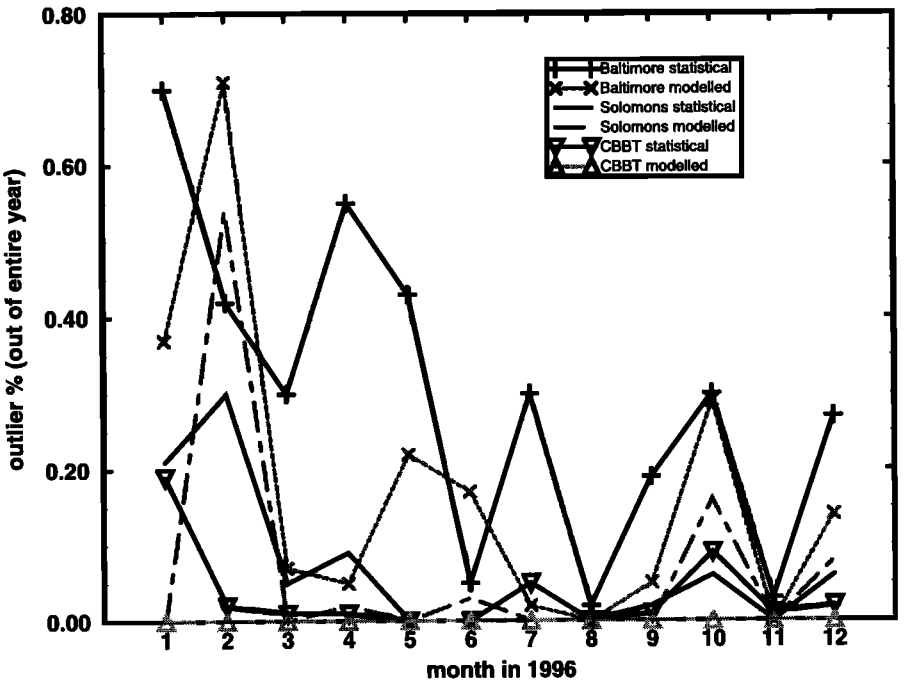

Figure 11b. Monthly variation of the outliers, shown as the percentage of differences between observed and hindcast subtidal water levels that exceeded 30 cm in absolute value. Data are for 1996.

Third, the spatial pattern in the variance contained in the wind-forced water levels is quite consistent between years. In the statistical hindcasts the wind-forced variance at Baltimore was ~3 times that at Solomons Island, and the variance at Solomons Island is approximately equal to that at CBBT. This pattern of spatial variation also corresponds to that produced by the EOF analysis (Figure 5). In the model hindcasts the wind-forced variance at Baltimore was also ~3 times the variance at Solomons Island. However, the modeled variance was extremely small at CBBT; the wind-forced variance there may be artificially small because of the proximity of the ocean boundary condition which limits the action of the wind.

Fourth, at Solomons Island and Baltimore both methods show that the variance in the total hindcast subtidal signal is less than the sum of the variances in the wind-driven and the coastally driven signals. This inequality supports the concept that when the forcings are operating simultaneously, the coastal signal and the wind signal tend to partially compensate each other. The compensation is greater in the upper Bay (also see Figure 3). For example, this compensation could occur during northerly winds when setdown in the upper Bay would be to some extent counteracted by a positive, coastally induced setup caused by Ekman forcing on the shelf just outside the bay's entrance.

6.4. Relative Magnitudes of Coastally Driven and Wind Driven Variations

An attempt was made to quantify the ratio of the coastally forced to the wind-forced variability. Only a few approaches have been proposed in the literature which can be used objectively to quantify this ratio, and we review them here briefly. Using some of these approaches, we have developed four methods for estimating the ratio, and these are explained below. The first approach was described by *Garvine* [1985]; we refer to this approach in method 1 and discuss it further

Table 4. Variance of the Subtidal Water Level Variation at Three Chesapeake Bay Stations.

Water Level Component, Origin	1994			1996		
	Bal	Sol	CBBT	Bal	Sol	CBBT
Total, observed	330.4	233.3	290.4	400.1	248.7	252.6
Total, statistical hindcast	215.4	172.0	242.3	248.3	171.4	215.5
Coastal only, statistical hindcast	152.2	154.7	161.6	153.3	156.0	163.2
Wind only, statistical hindcast	120.3	41.7	55.7	183.3	73.8	46.9
Total, modeled hindcast	276.7	245.8	382.4	300.9	227.4	331.4
Coastal only, modeled hindcast	361.7	348.6	361.1	298.7	292.9	311.4
Wind only, modeled hindcast	217.4	58.6	2.3	280.2	84.5	2.2

The results are for the observed total and both statistical and numerical model-generated hindcasts of total, coastally forced, and wind-forced variations. Note that the variance of the observed minus the variance of the predicted does not generally equal the variance of the error (Table 3), which is the variance of predicted minus the observed. Bal, Baltimore, Sol, Solomons Island.

Table 5. Estimates of the Ratio of the Subtidal Water Level Variance Due to Local Wind Forcing to the Subtidal Water Level Variance Due to Coastal Forcing at Three Chesapeake Bay Stations Using the Four Methods Discussed in the Text and Data for 1996.

Method	Baltimore	Solomons Island	CBBT
Analytical model (method 1)	1.68	0.60	<0.01
EOF analysis (method 2)	0.70	0.17	0.19
Ratios of prediction terms (method 3)	0.65	0.38	0.29
Ratios from variance, statistical hindcast (method 4)	1.20	0.47	0.29
Ratios from variance, model hindcast (method 4)	0.94	0.29	0.01
Average of all methods	1.03	0.38	0.16

below. Another approach was used by *Wong and Moses-Hall* [1998], who solved the same equations as *Garvine* [1985] but obtained a solution that was a function of frequency. They quantified the importance of wind and coastal forcing in Delaware Bay as the product of two quantities; the first was the ratio of the amplitude of the coastal setup to the amplitude of wind stress along the bay, and the second was the ratio of the respective low-frequency transfer functions. For the amplitudes they used the standard deviation of the observed water level and wind stress signals. Although we do not attempt to derive transfer functions for Chesapeake Bay, we will use the standard deviations as inputs in one of our methods (method 3). In the third approach, *Paraso and Valle-Levinson* [1996] estimated the relative importance of not coastal and wind-driven components but atmospheric pressure relative to wind stress in subtidal water levels at the entrance to Chesapeake Bay. Their results were based on determining the maximum value of the ratio of the pressure component to the total variation during a limited number of extreme events. We did not use this approach because it is event-oriented, and we seek a result that is representative of average conditions.

For method 1 we used *Garvine's* [1985] analytical results for a bay that is small relative to the subtidal wavelength but with quantities appropriate to Chesapeake Bay (Coriolis parameter = 0.9 x 10^{-5} s^{-1}, RMS coastal water level fluctuation = 17.0 cm, RMS wind stress = 0.88 dyn cm^{-2}, and the ratio of the product of RMS coastal water level fluctuation and Coriolis parameter to the RMS wind stress = 2.76 x 10^{-4} cm^3 dyn^{-1} s^{-1}) and assumed distances from the entrance for CBBT, Solomons Island, and Baltimore of 10, 150, and 250 km, respectively. For each of the three locations, we computed the amplitudes of the coastally forced and the wind-forced terms for 36 wind directions, equally spaced at 10°. The sign of the coastally forced term is always opposite that of the wind-forced term, which is consistent with a wind setup and coastal setup acting in opposition. Then, for each location we computed the variance of each of the terms and then the ratio of the two variances. The results are shown in Table 5.

Three additional methods were developed using the data and hindcast methods described in this paper. Method 2 was based on the results of the EOF analysis. Assuming that the first mode is due entirely to the coastal forcing and the second is due entirely to wind forcing, we calculated the ratio of the percentage of the total variability (based on the energy shown in Figure 6) in the second mode to the percentage in the first mode at Baltimore, Solomons Island, and CBBT (Table 5).

For method 3 we determined the ratios of the magnitudes of the local wind and the coastal terms using the statistical prediction equations, but, following *Wong and Moses-Hall* [1998], for input we used the variances (the square of the standard deviations shown in Table 6) of the input variables in 1996 rather than the hourly values. The hindcast equations ((1)-(3)) clearly show the separate contributions of the local wind and the coastal effect. For example, for the subtidal water level at Baltimore the coastal term is the product of 0.700 and 0.177^2 m^2, or 0.0219 m^2. The wind terms are 0.0070 m^2 and 0.0072 m^2. Hence the sum, 0.0142 m^2, is 0.65 times the size of the coastal term. Results for the three stations are shown in Table 5.

Method 4 is based on comparing the variance of our hindcast water level signals using hourly values in 1996 generated by each method when either one or the other forcing was turned off (see Table 4). For example, using the statistical hindcast, we find that at Baltimore the variance due to wind forcing alone is 183.3 cm^2 and that due to coastal forcing alone is 153.3 cm^2, so the ratio of the variances due to wind forcing and coastal forcing is 1.20. Results using both statistical and model-based hindcasts are shown in Table 5.

In general, the results from each method are consistent with each other and indicate that ratio of the variability due to direct wind forcing to the variability due to coastal forcing is a minimum at CBBT (averaging 16%) and increases with distance up the bay to 38% at Solomons Island and to 103% at Baltimore. There are some differences between the methods. The results from EOF analysis (method 2) give a ratio of wind component to coastal component at Baltimore lower than any other method and do not show the pattern of the ratio steadily increasing with distance up the bay. The model-based hindcasts (method 4) give the lowest ratio at CBBT because that location is close to the model's boundary cells and is therefore overwhelmingly influenced by the coastal setup.

7. Summary And Conclusions

7.1. Summary

We have developed and evaluated two methods of hindcasting water levels for the Chesapeake Bay. One was based on a (statistical) linear regression analysis, and the other was based on a numerical circulation model. We used two full years of hourly water level and wind data; 1994 data were used to develop each hindcast method, and 1996 data were used for validation. For the statistical hindcast, predictors of subtidal water levels were the subtidal water level at Lewes and wind stresses along certain directions at locations in the lower bay (CBBT) and the upper middle bay (Thomas Point). The specific wind direction for each meteorological station was

Table 6. Standard Deviation of the Variables Used to Evaluate the Statistical Hindcasts ((1)-(3)) for 1996 using Method 3.

Variable	Standard Deviation
η_L	0.177
T_{C050}	0.094
T_{C130}	0.080
T_{C140}	0.084
T_{T050}	0.065
T_{T140}	0.090

η_L is the subtidal water level at Lewes (m) and T is the wind stress per unit density (m^2/s^{-2}). For the wind stress the subscript denotes either Thomas Point (T) or CBBT (C) and the direction from which the wind comes.

chosen to give the highest correlation with water levels. The coastally forced water level was computed by applying the regression equation using the Lewes subtidal water level but with zero winds. The wind-forced water level was computed by applying the regression equation using the wind inputs but a zero Lewes subtidal water level.

The numerical circulation model was run in two-dimensional, barotropic mode and was forced by an ocean boundary water level, wind stress, and river flows. The ocean boundary water level was computed as a constant times the water level observed at CBBT a few tenths of an hour later (the observed water level at CBBT contains both astronomic tide and a subtidal component that originates primarily from the local continental shelf). A wind field was generated from observed winds at two locations. Because the model contains nonlinear terms, the subtidal water levels were generated by subtracting the time series produced by the model with either wind or coastal subtidal forcing removed from a times series made with all forcings.

7.2. Accuracy of Each Hindcast Method

The accuracy of the two hindcasting methods was evaluated by first comparing the results of each method with water level observations at the three proxy locations. Accuracy was characterized by RMS differences and outliers (defined as the percentage of time that the error exceeded 30 cm), each computed for both annual and monthly periods. For both methods, errors were lowest at CBBT and increased with distance from the entrance, most likely because the locations became more distant from the location of the coastal forcing station where the water level was observed. On the basis of a comparison of both differences and outliers for 1996 the model-based hindcasts were slightly more accurate than the statistically based hindcasts at all three locations (Table 2). The analysis of the seasonal variability of the differences revealed that errors are higher than average in winter and lower than average in summer. Also, although the annual RMS of the model is lower at all stations, there are months in which the statistical method is superior. Both the statistical equations and the numerical model had the most difficulty in reproducing water levels during wind-dominated events that began with winds from the south and ended with winds from the north. During these events both local winds and the coastal wave are important, and there is some compensation. However, the statistical model's coefficients are forced to assume that each effect is independent. The numerical model should simulate the compensation, but in the simulations the upper bay did not drain as rapidly as the observations indicated.

7.3. Coastally Driven and Wind Driven Variations

We used the observations and the hindcasts to analyze and quantify the role of coastal forcing relative to that of wind forcing. The variance contained in both the statistical and model-based hindcasts of coastally forced water levels imply that the long-period coastal wave undergoes very little change as it propagates up the bay. The statistical hindcast equations also indicate that coastal wave progresses at ~8-10 m s^{-1}, the shallow-water wave speed. In comparison, the amplitude of the astronomic tide wave is significantly altered during propagation within the bay owing to reflection at the head and bottom friction [*Browne and Fisher*, 1988].

In contrast for the coastally forced water level, the wind-forced water level was shown by all methods to be relatively small at the entrance, larger in the middle bay, and largest and about equal to the coastally forced water level in the upper bay. The use of both the statistical hindcasts and the model hindcasts in assessing the role of wind forcing and coastal forcing lends support to the concept that in Chesapeake Bay, when the forcings are operating simultaneously, the coastally driven water level variation and the wind-driven water level variation tend to partially compensate each other. Because the wind-forced water level increases in amplitude with distance from the entrance, the compensation is greater in the upper bay. For example, this compensation would occur during northerly winds when setdown in the upper bay would be partially counteracted by a positive, coastally induced wave caused by Ekman forcing on the shelf just outside the bay's entrance (see Figure 3), leading to a smaller subtidal water level signal than if only one of the forcings had been active. It appears that this compensation occurs during a significant number of events throughout the year, often enough to make the separation of coastal forcing and wind forcing difficult. The implication for hindcasting and forecasting is that errors in specifying the wind field and/or errors in specifying the coastally forced wave will lead to errors in the subtidal water level in the upper bay because the extent of compensation of the two effects will not be correct.

7.4. Future Plans

NOS plans to implement an operational nowcast/forecast system in Chesapeake Bay using the numerical model described herein. The system will be based on the numerical circulation model because it is more accurate in hindcast mode than the statistical prediction and it can more easily incorporate forecast winds over the bay. Present research is focusing on the data assimilation of water levels and winds to improve the accuracy of the simulations. Improvements in the present model's capabilities could be made with the use of a grid with higher spatial resolution and with the expansion of the model to three dimensions. Another area of research would involve recalibration of the model to change its water level response to more closely match the spectra of the observed water levels (Figure 9). These would include altering the value of α in determining the coastal boundary water level condition (see (5)), and increasing the wind drag coefficients (see (4)). Preliminary efforts have been made in two areas: using observed water levels at Kiptopeke in developing the coastal boundary condition and employing different amplitude factors and phase lags for the tidal and the subtidal components of the water level. Neither of these modifications resulted in significantly more accurate hindcasts.

Acknowledgments. The authors would like to thank Bruce Parker for his support of forecasting Chesapeake Bay water levels and Chris

Zervas, who provided the spectral plotting and the EOF analysis routines. Extremely helpful reviews of the draft were provided by Frank Aikman, John Kelley, Tom Gross, and Jye Chen, Curt Loy, Mark Bushnell, and Guy Noll (all from NOAA) and Larry Atkinson, Old Dominion University and two anonymous reviewers. K.T. Bosley is grateful to Old Dominion University's Center for Coastal Physical Oceanography for providing office facilities and for a productive work environment which encourages collaborative research.

References

Blumberg, A. F, Numerical tidal model of Chesapeake Bay, *J. Hydraul. Eng., 103* (HY1), 1-10, 1977.

Blumberg, A. F., The influence of density variations on estuarine tides and water levels, *Estuarine Coastal Mar. Sci.,6*, 209-215, 1978.

Bosley, K. T., and K. W. Hess, Development of an experimental nowcast/forecast system for Chesapeake Bay water levels, in the *4th International Conference on Estuarine and Coastal Modeling*,pp. 413-426, Am. Soc. of Civ. Eng., New York, 1998.

Brooks, D. A., A model study of the buoyancy-driven circulation in the Gulf of Maine, *J. Phys. Oceanogr. 24*(11), 2387-2412, 1994.

Browne, D. R., and C. W. Fisher, Tide and tidal currents in the Chesapeake Bay, *NOAA Tech. Rep. NOS OMA 3*, 84 pp + appendices, Nat. Ocean Serv. Office of Oceanogr. and Mar. Assess., Silver Spring, Md., 1988.

Elliot, A. J., Observations of the meteorologically induced circulations in the Potomac estuary, *Estuarine Coastal Mar. Sci., 6*, 285-299, 1978.

Elliot, A. J., and D.-P. Wang, The effect of meteorological forcing on the Chesapeake Bay: The coupling between an estuarine system and its adjacent coastal waters, *in Hydrodynamics of Estuaries and Fjords*, pp.127-145, Elsevier Sci., New York, 1978.

Garvine, R. W., A simple model of estuarine subtidal fluctuations forced by local and remote wind stress, *J. Geophys. Res , 90*, 11,945-11,948, 1985.

Hess, K. W., MECCA program documentation, *NOAA Tech. Rep. NESDIS 46*, 243 pp., Nat. Environ. Satell., Data, and Info. Serv. Natl. Oceanic and Atmos. Admin., Silver Spring, Md., 1989.

Hess, K.W., MECCA 2 program documentation, NOAA, Tech. Rep. *NOS CS 5*, 49 pp. Nat. Ocean Serv. Natl. Oceanic and Atmos Admin., Silver Spring, Md., 2000.

Hutchinson, G. E., *A Treatise on Limnology*, Vol. 1, *Geography, Physics, and Chemistry*, 1015 pp., J. Wiley, New York, 1957.

Johnson, B H., K. W. Kim, Y. P. Sheng, and R. E. Heath, Development of a three-dimensional hydrodynamic model of Chesapeake Bay, in *Proceedings, of the International Conference on Estuarine and Coastal Modeling*,. pp. 172-181, Am. Soc. of Civ, Eng., New York, 1990

Johnson, D. F., and K W. Hess, Numerical simulations of blue crab larval dispersal and recruitment, *Bull. Mar. Sci., 46*(1), 195-213, 1990.

National Ocean Service (NOS), NOS procedures for developing and implementing operational nowcast and forecast systems for PORTS, *NOAA Tech. Rep. NOS CO-OPS 20*, 33 pp., Natl. Oceanic and Atmos. Admin., Silver Spring, Md., 1999.

Paraso, M. C., and A. Valle-Levinson, Meteorological influences on sea level and water temperature in the lower Chesapeake Bay: 1992, *Estuaries, 19*(3), 548-61, 1996.

Pollak, M J., Axial slope of sea level in Chesapeake Bay, *EOS Trans., AGU, 38*(1), 62-64, 1957.

Pollak, M. J., Wind setup and shear stress coefficients in Chesapeake Bay, *J. Geophys. Res., 65*, 3383-3389, 1960.

Spitz, Y H., and J. M Klink, Estimate of the bottom and surface stress during a spring-neap tide cycle by dynamical assimilation of tide gauge observations in the Chesapeake Bay, *J Geophys. Res.,103*, 12,761-12,782, 1998.

Tag, P. M., F. W. Murray, and L. R. Koenig, A comparison of several forms of eddy viscosity parameterization in a two-dimensional cloud model, *J. Appl. Meteorol., 18*, 1429-1441, 1979.

Vieira, M. E. C., The meteorologically driven circulation in mid-Chesapeake Bay, *J. Mar. Res., 44*, 473- 493, 1986.

Walstad, L. J., G. J. Szilagyi, F. Aikman, L. C. Breaker, F. Klein, J. J. D'Aleo, and J. T. McQueen, The Coastal Marine Demonstration Project, in *Proceedings of the Sixth International Conference on Estuarine and Coastal Modeling*, pp 646-662, Am. Soc. of Civ. Eng., New York, 2000.

Wang, D.-P., Subtidal sea level variation in the Chesapeake Bay and relations to atmospheric forcing, *J. Phys. Oceanogr., 9*, 413-421, 1979a.

Wang, D.-P., Wind-driven circulation in the Chesapeake Bay, winter 1975, *J. Phys. Oceanogr., 9*, 564-572, 1979b.

Wang, D.-P., Low frequency sea level variability on the Middle Atlantic Bight, *J. Mar. Res.* 37, 683- 697, 1979c.

Wang, D.-P., and A. J. Elliot, Non-tidal variability in the Chesapeake Bay and Potomac River: Evidence for non-local forcing, *J. Phys. Oceanogr., 8*, 225-232, 1978.

Willmott, C. J., S. G. Ackleson, R. E. Davis, J. J. Feddema, K. M. Klink, D. R. Legates, J. O'Donnell, and C. M. Rowe, Statistics for the evaluation and comparison of models, *J. Geophys. Res. 90*, 8995- 9005, 1985.

Wong, K.-C., and J. E. Moses-Hall, On the relative importance of the remote and local wind effects to a subtidal variability on a coastal plain estuary, *J. Geophys. Res., 103*, 18,393-18,404, 1998

Wu, J., Wind-stress coefficients over sea surface under neutral conditions-A revisit, *J. Phys. Oceanogr., 10*, 727-740, 1980.

Zervas, C. E., A water level forecasting system for Tampa Bay, Florida, paper presented at Conference on Coastal Oceanic and Atmospheric Prediction, Am. Meteorol. Soc., Atlanta, Ga., Jan. 28 to Feb. 2, 1996.

K. T. Bosley, Center for Operational Products and Services, NOAA, Crittenton Hall, Old Dominion University, 768 Fifty-Second Street, Norfolk, VA 23529. (Bosley@ccpo.odu.edu)

K. W. Hess, Office of Coast Survey, National Ocean Service, NOAA, 1315 East-West Highway, Room 7826, Silver Spring, MD 20910. (Kurt.hess@noaa.gov)

(Received January 17, 2000; revised February 9, 2001; accepted March 21, 2001.)